

1 **Implementation and validation of a Wilks-type multi-site**
2 **daily precipitation generator over a typical Alpine river**
3 **catchment**

4
5 **D. E. Keller^{1, 2, 3}, A. M. Fischer¹, C. Frei¹, M. A. Liniger^{1, 3}, C. Appenzeller^{1, 3}, R.**
6 **Knutti^{2, 3}**

7 [1] {Federal Office of Meteorology and Climatology MeteoSwiss, Operation Center 1, 8085
8 Zürich-Flughafen, Switzerland}

9 [2] {Institute for Atmospheric and Climate Science, ETH Zürich, Universitaetstrasse 16, 8092
10 Zurich, Switzerland}

11 [3] {Center for Climate Systems Modeling (C2SM), ETH Zurich, Universitaetstrasse 16,
12 8092 Zurich, Switzerland}

13 Correspondence to: D. E. Keller (Denise.Keller@meteoswiss.ch)

14
15 **ABSTRACT**

16 Many climate impact assessments require high-resolution precipitation time-series that have a
17 spatio-temporal correlation structure consistent with observations, for simulating either
18 current or future climate conditions. In this respect, weather generators (WGs) designed and
19 calibrated for multiple sites are an appealing statistical downscaling technique to
20 stochastically simulate multiple realizations of possible future time-series consistent with the
21 local precipitation characteristics and its expected future changes. In this study, we present the
22 implementation and validation of a multi-site daily precipitation generator re-built after the
23 methodology described in Wilks (1998). The generator consists of several Richardson-type
24 WGs run with spatially correlated random number streams. This study aims at investigating
25 the capabilities, the added value and the limitations of the precipitation generator for a typical
26 Alpine river catchment in the Swiss Alpine region under current climate.

27 The calibrated multi-site WG is skilful at individual sites in representing the annual cycle of
28 the precipitation statistics, such as mean wet day frequency and intensity as well as monthly

1 precipitation sums. It reproduces realistically the multi-day statistics such as the frequencies
2 of dry and wet spell lengths and precipitation sums over consecutive wet days. Substantial
3 added value is demonstrated in simulating daily areal precipitation sums in comparison to
4 multiple WGs that lack the spatial dependency in the stochastic process. Limitations are seen
5 in reproducing daily and multi-day extreme precipitation sums, observed variability from year
6 to year and in reproducing long dry spell lengths. Given the performance of the presented
7 generator, we conclude that it is a useful tool to generate precipitation series consistent with
8 the mean climatic aspects and likely helpful to be used as downscaling technique for climate
9 change scenarios.

10 **1 Introduction**

11 In Switzerland, precipitation is a key weather variable with high relevance for sectors such as
12 energy production, infrastructure, tourism, agriculture and ecosystems. Owing to a complex
13 topography, daily precipitation varies strongly in space and time (Frei and Schär, 1998; Isotta
14 et al., 2013). The spatial distribution of daily precipitation frequency and intensity depends on
15 the topography, with higher frequencies and intensities along the North-Alpine ridge during
16 summer, and a strong north-south gradient with heavier intensities in southern Switzerland
17 from spring to autumn. The most prominent weather situations causing these precipitation
18 patterns are shallow pressure systems favouring convective precipitation, orographically
19 induced precipitation (e.g. Föhn situations), and frontal passages. Precipitation amounts and
20 frequencies are typically largest in summer, mainly due to convective processes (Frei and
21 Schär, 1998).

22 Given the expected changes in the hydrological cycle over the 21st century (Allen and
23 Ingram, 2002; Held and Soden, 2006), the need for reliable and quantitative future local
24 precipitation projections in Switzerland is continuously growing. To effectively assess the
25 impacts related to changes in precipitation, often highly localized daily data are needed that
26 are ideally both consistent in time and in space (e.g. Köplin et al., 2010). Currently, in
27 Switzerland various impact assessment reports rely on the statistically downscaled
28 precipitation change data derived from regional climate models by the well-known and simple
29 delta change approach, which shifts an observed time series by a model-derived change in the
30 mean climate (BAFU, 2012; Bosshard et al., 2011; CH2014-Impacts, 2014). The delta change
31 approach accounts for changes in the mean annual cycle, but potential changes in inter-annual

1 variability, changes in wet-day frequency and intensity or of spell lengths are not taken into
2 account. Hence, the data are also not suitable for the analysis of future changes in extreme
3 events (Bosshard et al., 2011). It is our aim here to develop a statistical downscaling method
4 for Switzerland that overcomes some of these limitations and that subsequently can be easily
5 applied to climate model output.

6 Over recent years a vast number of statistical downscaling methods have been developed that
7 go far beyond a simple delta change approach (Maraun et al., 2010). These include bias-
8 correction methods (e.g. Themeßl et al., 2011), regression-based methods (e.g. Hertig and
9 Jacobeit, 2013) or weather generator (WG) approaches (e.g. Chandler and Wheeler, 2002;
10 Mezghani and Hingray, 2009). For our purposes, the latter method is especially appealing,
11 since it includes a stochastic component. This is a major improvement compared to a
12 (deterministic) delta change approach, allowing to investigate multiple time-series and
13 uncertainty at the local scale that are consistent with a given (current or future) mean climate.
14 Moreover, it allows the incorporation of changes in the temporal correlation structure and
15 consequently alterations of the dry-wet sequences. From an agricultural impact (e.g. Calanca,
16 2007) or water resource management's (e.g. Samuels et al., 2009) perspective this is a key
17 aspect of future precipitation change.

18 A serious limitation of many WGs is that they are often calibrated to observations at single
19 sites only, therefore lacking the spatial correlation structure that is required for many
20 applications, particularly in the context of hydrological impact modelling in a topographically
21 complex terrain such as the Alps. A number of sophisticated approaches in time-space
22 precipitation simulation have been put forward in the literature to address this issue, such as
23 K-nearest neighbor resampling approaches (e.g. Buishand and Brandsma, 2001), copula based
24 approaches (e.g. Bárdossy and Pegram, 2009), Poisson cluster models (e.g. Cowpertwait,
25 1995; Fatichi et al., 2011) or more sophisticated field generators (e.g. Paschalis et al., 2013;
26 Peleg and Morin, 2014). Of increasing popularity are Markovian multi-site models (e.g.
27 Baigorria and Jones, 2010; Wilks, 1998) and in particular non-homogeneous hidden Markov
28 model (NHMMs) (e.g. Bellone et al., 2000; Hughes et al., 1999; Kioutsioukis et al., 2008;
29 Robertson et al., 2004, 2009). The latter approach models transitions between pre-defined
30 precipitation state patterns conditional on the synoptic-scale circulation. Each of these time-
31 space WGs come with method-specific benefits and limitations for the reproduction of the
32 daily precipitation statistics and consequently its use in impact models. For instance, some of

1 them do better in simulating more realistically longer-term variability (e.g. generalized linear
2 model (GLM) based multi-site WGs, Chandler, 2014), while some are explicitly adapted to
3 deal with extreme precipitation (e.g. Huser and Davison, 2014).

4 The main purpose of our precipitation generator is its use as a downscaling tool in a climate
5 change context. It should be easily transferable to different climatological regions and time-
6 periods and its generated time-series should serve several impact applications that have
7 different needs in terms of time-space consistency. For these reasons we opt for a
8 precipitation generator whose degree of complexity and associated calibration requirements
9 are still sufficiently easy to handle. Mehrotra et al. (2006) inter-compared three stochastic
10 multi-site precipitation occurrence generators over a region over Australia and found that the
11 generator by Wilks (1998) outperforms Hidden Markov models and K-nearest neighbour
12 resampling techniques in terms of overall performance, time required for model running and
13 simplicity of the model structure. Hence the multi-site precipitation generator proposed by
14 Wilks (1998) therefore serves our purposes. It is a relatively simple tool based on a
15 Richardson-type WG (Richardson, 1981) run with spatially correlated random number
16 streams.

17 It is the aim of this study to investigate the capabilities, the added value and the limitations of
18 this multi-site generator in order to better interpret the climatic changes in the simulated time-
19 series for a future climate, which is part of an upcoming study. In particular, the actual
20 amount of stochastically generated variability will be assessed as well as the added value of a
21 multi-site model against multiple single-site models. The analysis is done for the Swiss
22 catchment *Thur*. While being not of the same level of familiarity as other catchments, the
23 *Thur* catchment serves as an ideal testbed for our purposes, as will be detailed in Sect. 2. In
24 Sect. 3 we recapitulate the basic procedures to multi-site precipitation simulation after Wilks
25 (1998) and detail how the generator was calibrated over the catchment. Results of the
26 validation against observations and against single-site generators will be presented in Sect. 4.
27 We end the article with a discussion (Sect. 5) and a summary and outlook (Sect. 6).

28 **2 Selection of catchment area**

29 This study focuses on the hydrological catchment of the river *Thur* (located in the north-
30 eastern part of Switzerland, Figure 1a) that is a feeder river of the Rhine with a length of
31 about 135 km and a catchment area of approximately 1696 km². Its flow regime is nivo-

1 pluvial that is heavily influenced by snowmelt (BAFU, 2007). Mean annual rainfall amounts
2 to approximately 900 mm in the lowlands with 120 wet days per year. At the mountain station
3 *Saentis*, up to 2900 mm fall in an average year on about 170 wet days. Approximately one
4 third of the precipitation accumulates as snow at higher stations in the mountains, whereas in
5 the lowlands less than 10% of the annual sums fall as snow. This particular catchment was
6 selected for mainly two reasons:

- 7 (a) In an upcoming study our generated synthetic time-series over the Thur catchment will
8 serve as input to two hydrological models to assess the runoff regime under current and
9 future climate (similar as in Jasper et al., 2004). The *Thur* is a well-studied and well-
10 observed river catchment in Switzerland (e.g. Fundel et al., 2013; Kunstmann et al.,
11 2006) providing high-quality hydrological measurement series for a robust calibration of
12 hydrological runoff models. It further represents the largest Swiss river without a natural
13 or artificial reservoir and therefore exhibits discharge fluctuations similar to unregulated
14 Alpine rivers.
- 15 (b) Owing to the complex topography over this catchment area (ranging from less than 400
16 meters a.s.l. to more than 2500 meters a.s.l.), precipitation exhibits a large variability both
17 in space and in time (see Figure 1b and 1c based on gridded observational data from Frei
18 and Schär (1998)). Over 1961-2011 and for a winter and summer month, the data clearly
19 show larger precipitation frequencies and intensities over higher-elevated regions
20 compared to the lowlands. A large portion of these precipitation characteristics can be
21 explained by a north-east to south-west lying mountain range (*Alpstein*) extracting
22 precipitation from westerly flows and triggering convective storms. These spatio-
23 temporal variations serve hence as an ideal observation basis to validate and analyse the
24 capabilities and limitations of the WG.

25 For the purpose of this study, we selected eight evenly distributed measurement stations
26 (Figure 1a) of MeteoSwiss that all provide homogenized time-series covering a 51-year
27 period from 1961-2011 (Begert et al., 2003), and that sufficiently cover the elevation profile
28 of the catchment area.

1 **3 Method**

2 **3.1 Precipitation occurrence and amount model**

3 The core of our multi-site WG is a Richardson-type precipitation generator (Richardson,
4 1981) consisting of an occurrence and amount model. To model occurrence at a single station
5 we rely on a first-order two-state Markov chain (Gabriel and Neumann, 1962; Richardson,
6 1981; Wilks and Wilby, 1999). The use of a first-order model in our WG was justified by
7 inspecting the Akaike information criterion (AIC) (Akaike, 1974) and the Bayesian
8 information criterion (BIC) (Schwarz, 1978). Both criteria revealed a substantial
9 improvement when going from a zero-order to a first-order model, but the additional gain at a
10 second- or higher-order model was negligible (not shown). We used a specific wet-day
11 threshold of 1 mm day⁻¹ to discretize a given daily precipitation time-series $X(t)$ at a given site
12 into the two states ‘dry’ ($X(t) < 1 \text{ mm day}^{-1}$, $J_t = 0$) and ‘wet’ ($X(t) \geq 1 \text{ mm day}^{-1}$, $J_t = 1$). The
13 wet-wet (p_{11}) and dry-wet (p_{01}) transition probabilities suffice to fully specify the first-order
14 two-state Markov chain model:

$$15 \begin{aligned} p_{11} &= P\{J_t = 1 | J_{t-1} = 1\} \\ p_{01} &= P\{J_t = 1 | J_{t-1} = 0\} \end{aligned} \quad (1)$$

16 For an estimate of the transition probabilities we rely on their conditional relative frequencies
17 (Wilks, 2011). Other important precipitation indices can be inferred. The wet day frequency
18 (wdf, π) is defined as the ratio of the number of wet days to the total number of days over a
19 given time period:

$$20 \quad \pi = \frac{p_{01}}{1 + p_{01} - p_{11}} \quad (2)$$

21 Similarly, the lag- k autocorrelation r_k is defined as:

$$22 \quad r_k = (p_{11} - p_{01})^k \quad (3)$$

23 Since day-to-day precipitation generally exhibits positive serial correlation (i.e. $r_1 > 0$), p_{11} is
24 usually larger than p_{01} and the wdf is between the two. Note, that a first-order Markov chain
25 does not imply independence for lags greater than one. The autocorrelation r_k (equation (3))
26 decays exponentially with larger lags k .

1 Given a simulated wet day from the occurrence model, precipitation amounts are set. This is
2 done by sampling from a mixture model of two exponential distributions (Wilks, 1999a):

$$3 \quad f(x) = \frac{w}{\beta_1} \exp\left(-\frac{x}{\beta_1}\right) + \frac{1-w}{\beta_2} \exp\left(-\frac{x}{\beta_2}\right) \quad (4)$$

4 $f(x)$ is a weighted average (weight w) of two exponential distributions with means β_1 and β_2 .
5 The parameters w , β_1 and β_2 are estimated based on maximum-likelihood (Tallis and Light,
6 1968). Note that the estimation of PDF parameters is subject to sampling uncertainty from the
7 available number of wet days in a given calendar month.

8 **3.2 Stochastic modelling of multi-site daily precipitation**

9 The simulation process is based on Richardson (1981) at single stations with the five above-
10 introduced parameters: i.e. the transition probabilities p_{11} and p_{01} as well as w , β_1 and β_2 . That
11 is, a uniform random number between 0 and 1 is compared to either p_{11} or p_{01} depending on
12 the state of the previous day and correspondingly set as either dry or wet. In case of a wet day,
13 a second uniform random number is drawn to assign the precipitation amount based on the
14 quantile function. For further details on the simulation of precipitation at a single location we
15 refer to Wilks and Wilby (1999) and to the Supplementary Material. The simulation allows
16 time-series of arbitrary length resembling observed climatological precipitation statistics, both
17 in terms of frequency and intensity.

18 The main extension to a multi-site model after Wilks (1998) is to drive several single-site
19 WGs simultaneously with spatially correlated but serially independent random numbers. To
20 generate correlated random number streams, we rely on a Cholesky decomposition (e.g.
21 Higham, 2009). The latter requires matrices that are positive definite, which is not always
22 granted. In absence, a fall-back solution based on the nearest positive correlation matrix is
23 chosen (e.g. Higham, 1989). This problem, however, occurs only a few times in our study.
24 One of the main hurdles in simultaneously generating precipitation at multiple sites is to
25 ensure that the spatial dependence is also preserved in the final generated time-series (Wilks
26 and Wilby, 1999; Wilks, 1998). This difficulty mainly arises from the stochastic process that
27 partly destroys the initially imposed correlation structure again (Wilks, 1998). To circumvent
28 this problem, Wilks (1998) suggested an optimization procedure based on a bisection method
29 (Burden and Faires, 2010) that minimizes the difference between the generated spatial

1 correlation and the target correlation of observations. In our case, the iteration is repeated
2 until a precision of 0.005 is reached. This estimation procedure is done prior to the actual
3 simulation and has to be done for each station pair and each month. For further details
4 regarding the setup of stochastic simulation and in particular the implementation of multi-site
5 simulation we refer to the Supplementary Material.

6 **3.3 Implementation**

7 **3.3.1 Implementation of the multi-site WG over the *Thur* catchment**

8 The precipitation generator is calibrated on a monthly basis. First, all the single-site input
9 parameters (p_{11} , p_{01} , β_1 , β_2 and w) were estimated for each of the 8 stations within the
10 catchment and for each month separately using a time-window of 51 years (1961-2011). In
11 this study we chose a relatively long calibration period in order to minimize the effect of
12 sampling uncertainties. This allows us to accurately assess the added value of a multi-site
13 model against multiple single-site models and to better quantify systematic biases of the WG.
14 For the two transition probabilities in a given month, the climatological mean over the 51
15 yearly values of p_{11} and p_{01} was taken. In the case of fitting a PDF to non-zero precipitation
16 amounts and the estimation of β_1 , β_2 and w , we used the daily data over all 51 years together.
17 In addition, a three-month window centred at the month of interest was chosen, in order to
18 increase sample size and the robustness. The distributional parameters were derived based on
19 maximum-likelihood (Tallis and Light, 1968). Despite our three-month time-window, cases
20 occurred when the maximum-likelihood algorithm did not converge. For such cases, a fall
21 back solution was applied where the parameter estimates from the previous month were
22 adopted. With the monthly parameters from all the calibrated single-site WGs and the
23 monthly observed inter-station correlations (symmetric correlation matrices), the optimization
24 procedure for spatial correlation had to be applied (see Supplementary). In terms of a correct
25 temporal correlation in the generated time-series, it was ensured that the transitions between
26 adjacent months is continuous (i.e. the first day of a given month is conditioned on the last
27 day of the previous month). Note, that by calibrating the multi-site WG on a monthly instead
28 of a seasonal basis, additional sampling uncertainty is introduced due to the rather small time-
29 window to estimate our parameters. This is the downside of prescribing an improved annual
30 cycle in the WG parameters. Once the multi-site WG was calibrated, we generated 100

1 ensembles of daily time-series, of 51-year length. All the results presented in Sect. 4 are
2 calculated over the time-period 1961-2011.

3 3.3.2 **Reproduction and uncertainty of WG model parameters**

4 To test whether our WG is properly implemented, we evaluated the reproduction of WG input
5 parameters extracted from the generated time-series. A correct reproduction in parameters
6 such as wet day intensity, frequency and transition probabilities is a prerequisite for all the
7 subsequent analyses presented in Sect. 4. The evaluation was performed for four subjectively-
8 defined climatic regimes: a very dry, a dry, a wet and a very wet climate. The corresponding
9 model parameters are indicated in Figure 2 with dashed vertical lines. For each of these
10 precipitation regimes, 100 synthetic daily time-series were generated. To test the effect of
11 sample-size, different sizes of time-windows were used: (a) 10,000 days, (b) 1000 days, (c)
12 100 days and (d) 30 days. The latter corresponds to the same sample-size as for the simulation
13 of precipitation occurrence over the *Thur* catchment. For each of the generated time-series the
14 WG parameters were re-estimated and the 95% inter-quantile range was computed across the
15 set of 100 realizations (Figure 2). Three main results can be inferred: (a) our precipitation
16 generator is able to correctly reproduce the key WG parameters implying that the chances for
17 substantial coding errors are small; (b) as expected the estimate of the input parameters
18 becomes more uncertain for smaller sample sizes; in fact, the uncertainty range increases by a
19 factor of 18.3 when the sample size is reduced from 10,000 to 30. At a sample size of 1000
20 the uncertainty range stays at around ± 0.03 , that only marginally lowers when going to a
21 sample of 10,000. (c) the different pre-defined climate regimes affect the uncertainty,
22 particularly in the estimated transition probabilities. In a very dry or wet climate, the wet-wet
23 or dry-wet transition probability, respectively, exhibits large uncertainties in the estimate.
24 This again is mainly related to a sample size problem due to very few wet-wet or dry-wet
25 pairs. Thus, we expect that the weather generator does not work optimally in extremely wet or
26 arid climates.

27 **4 Results**

28 An in-depth evaluation of the generated time-series with our calibrated multi-site WG is now
29 undertaken with real observations. First, the reproduction of the daily and longer-term
30 precipitation statistics at individual sites is analysed (Sect. 4.1). In a second step, the
31 performance of the multi-site model is investigated regarding spatially aggregated

1 precipitation indices in comparison to WGs without incorporating spatial dependencies (Sect.
2 4.2).

3 **4.1 Validation of the precipitation generator at individual sites**

4 Based on our ensemble of synthetic time-series, each containing 51 years, we analyse the
5 reproduction of key precipitation characteristics. This validation goes beyond the
6 reproduction of pure model parameters used to calibrate the WG (Sect.3.3.2), as it includes
7 precipitation statistics that are not directly used in the specification and calibration of the
8 model. Note, that we present this analysis for the same time-period as used for calibrating our
9 WG. This is justified for the study here, as long as we treat and use our WG to simulate long-
10 term monthly precipitation statistics. In such a setup the stationarity of the model is given by
11 definition. However, in a climate prediction or projection context, this stationarity assumption
12 would have to be tested and hence separate calibration and validation periods are needed.

13 **4.1.1 Long-term mean and inter-annual variance of monthly precipitation sums**

14 In a first step of validating our WG, we focus on the reproduction of the long-term mean in
15 monthly precipitation sums. Figure 3 shows both the modelled (blue) and observed (black)
16 long-term monthly precipitation sum for each of the eight investigated stations. In general, the
17 annual cycle of precipitation sums is well reproduced. Consistently, this is also true for the
18 long-term seasonal as well as for the annual precipitation sums (not shown). But the WG
19 tends to slightly underestimate precipitation sums in June and August, and overestimate them
20 in October. In addition, the two stations *Bischofszell* (BIZ) and *Herisau* (HES) show rather
21 large positive deviations from the observed record during the winter months. In order to
22 explain part of these deviations, we decomposed the long-term mean of monthly ($T=30$ days)
23 precipitation sums ($E[S(T)]$) into the product of the mean monthly wet day frequency (wdf)
24 and intensity (wdi) (Figure 4):

$$25 \quad E[S(T)] = T \cdot wdf \cdot wdi \quad (5)$$

26 Since these two climatological quantities are indirectly forced (Sect. 3.3.2), we expect from
27 the results in Figure 2 a good match on average. As shown in Figure 4, this is true for the wet
28 day frequency, where the deviations between generated (red) and observed (black) values are
29 relatively small. The differences, however, are more pronounced in case of mean wet day
30 intensities. In fact, it is the wet day intensities that explain the mismatches in precipitation

1 sums. In case of the winter performance over *Bischofszell* and *Herisau* the deviations can be
 2 attributed to the failure of converging in case of fitting the non-zero precipitation amount. For
 3 those instances, the fallback solution had to be used (see 3.3.1).

4 Next we focus on the inter-annual variability of monthly precipitation sums, which is often
 5 more difficult to realistically model than the long-term mean (Wilks and Wilby, 1999). The
 6 shaded areas in Figure 3 represent the inter-quartile range of the observed (grey) and
 7 modelled (blue) monthly precipitation sums. From Figure 3 it is obvious that the variability of
 8 the WG is smaller than in observations for all of the analysed stations. This implies that the
 9 stochastic model only explains part of the observed total variability. This reduced variability
 10 is expected, as observations are subject to additional sources of variability, which our
 11 comparable simple WG is not trained for. The WG is forced with mean observed values,
 12 varying between months but not between different years. The annual cycle is assumed to be
 13 stationary, and hence interannual variability, e.g. related to the North Atlantic Oscillation
 14 (Hurrell et al., 2003) is missing. Consequently, the ratio of simulated over observed variance
 15 accounts for approximately 33% on average. The magnitude of this result is consistent with
 16 other studies (e.g. Gregory et al. 1993). Further insights can be gained from a decomposition
 17 of the variance of monthly ($T=30$ days) precipitation sums ($Var[S(T)]$) into the variance of
 18 non-zero amount ($Var[X \geq 1 \text{ mm day}^{-1}]$) and the variance of the number of wet days (Var
 19 $[N(T)]$) as proposed by Wilks and Wilby (1999):

$$20 \quad Var[S(T)] = T \cdot wdf \cdot Var\left[X \geq 1 \frac{mm}{d}\right] + Var[N(T)] \cdot wdi^2 \quad (6)$$

21 Since the mean wet day frequency (wdf) and intensity (wdi) are reasonably reproduced, we
 22 expect that the reduced variability of monthly precipitation sums originate from deficiencies
 23 in correctly reproducing the inter-annual variability of the number of wet days and/or of the
 24 non-zero amount. One likely reason is the neglect of low-frequency variability in the WG
 25 parameters. It has been shown that physically based models that include large-scale
 26 circulation as a predictor could alleviate this problem (Chandler and Wheeler, 2002; Furrer
 27 and Katz, 2007; Wheeler et al., 2005; Yang et al., 2005).

28 4.1.2 **Reproduction of PDF of daily non-zero amount**

29 The adequate reproduction of the mean wet day intensity and frequency is a necessary but not
 30 sufficient precondition of a WG to be used for subsequent (impact) studies. Due to a large

1 variability of precipitation amounts, it strongly matters how its frequency distribution is
2 reproduced. For this, we compared simulated and observed quantiles of the daily non-zero
3 precipitation distribution at each station (Supplementary Fig. 4). Generally, the mixture model
4 of two exponential distributions captures the frequencies of the intensities reasonably well,
5 even at the high-Alpine station *Saentis* (SAE). This is at least the case up to the 80th
6 percentile, above which intensities are systematically underestimated at all stations. This issue
7 could be overcome by more sophisticated amount models combining e.g. a Gamma with a
8 Generalized Pareto distribution (Vrac and Naveau, 2007).

9 4.1.3 **Reproduction of multi-day statistics**

10 While the frequencies of precipitation amounts and the frequencies of wet and dry days are
11 realistically simulated, it remains unclear how the WG performs for multi-day spells. For
12 many application studies, this is an essential information that requires a specific analysis.
13 Figure 5 displays observed and modelled cumulative frequencies of dry and wet spells lengths
14 at the example of two months and two stations. The two stations *Saentis* and *Andelfingen* are
15 selected for display since they represent the stations with the highest and lowest elevation in
16 the catchment. For both stations a clear seasonal difference in the probability of dry spells
17 toward more short and less long dry spells during summer compared to winter is found. A
18 plausible explanation are the more intermittent (convective) precipitation systems during
19 summer. In contrast to dry spells, no seasonal differences in wet spell length probabilities can
20 be inferred. This is likely related to the fact that the dry-dry transition probability p_{00} exhibits
21 a more distinct annual cycle than the wet-wet transition probability p_{11} . Figure 5 also shows
22 that the frequency at shorter spell lengths (up to 3 days) is more realistically reproduced by
23 the model than the frequency at longer spell lengths. Generally, a better reproduction of wet
24 spell probabilities is seen compared to the dry spell counterpart. Long dry spell lengths are
25 more frequently underestimated by the model than longer wet spell lengths. The
26 underestimation of long wet and dry spells is a common shortcoming of the Richardson-type
27 weather generator and has been reported by many studies before (e.g. Racsco et al. 1991).
28 This deficiency mainly arises due to the fast exponential decay of the autocorrelation function
29 with larger lags (see Eq. (3)). Similar to the underestimation of variability in precipitation
30 sums, higher-order Markov chains (Wilks, 1999b) or GLMs with additional predictors might
31 improve this aspect, which is out of scope in this study here.

1 Given that the frequency of wet spell lengths is realistically simulated, the question arises
2 whether this also holds for multi-day precipitation sums. Multi-day periods of rain is a
3 common phenomenon over Switzerland, especially during prevailing weather situations that
4 favour orographic uplift. We compared observed and simulated cumulative distribution
5 functions (CDFs) of precipitation sums over multiple consecutive wet days (Figure 6).
6 Overall, we found that the differences between generated and observed time-series are largest
7 for the higher quantiles and for long lasting wet spells (5-day wet spells) where the WG tends
8 to underestimate large multi-day sums. This reduced skill in simulating longer wet spell sums
9 can be explained by the fact that our WG is only prescribed with the temporal structure of
10 precipitation occurrence but not in amount. In other words, the WG has memory to
11 realistically reproduce multi-day wet spell lengths (Figure 5), while the combined analysis of
12 multi-day occurrence and accumulated amount loses somewhat this memory again. Two
13 further noticeable features in Figure 6 are that intense one-day precipitation sums are often
14 overestimated by the model compared to the observations, while a relatively good match is
15 obtained for three-day sums. Although the deficiency in correctly simulating multi-day sums
16 of consecutive wet days is to be expected by construction of the WG, it could be improved by
17 more sophisticated precipitation models, such as multi-state Markov-chains with different
18 probability density distributions conditioned on pre-defined states as for instance ‘dry’, ‘wet’,
19 ‘very-wet’ (Boughton, 1999; Gregory et al., 1993).

20 **4.2 Performance of spatial precipitation indices**

21 Up to this point we evaluated the generator at individual sites only. One of the key issue of
22 this study though is the potential added value of incorporating inter-station dependencies.
23 Similarly as in the previous section, we analyse the performance first in terms of occurrence-
24 related statistics and second in terms of the combined occurrence and amount statistics.

25 **4.2.1 Dry and wet spell statistics for the whole catchment**

26 Based on the eight stations in our catchment with each being either in a wet or dry state at a
27 given day, theoretically 2^8 (=256) different dry-wet patterns in space are possible. In
28 observations, though, it turns out that 70% of the investigated days over 1961-2011 are in fact
29 either completely dry (45%) or completely wet (25%) and the remaining 254 dry-wet-patterns
30 are subject to far smaller frequencies (around 10^{-5} - 10^{-3} %). The pre-dominance of a dry or a
31 wet catchment makes sense given that the catchment is relatively small and given that

1 precipitation is to a large degree circulation-triggered. Analysing the synthetic time-series
2 from our multi-site WG reveals an almost perfect match with observations (Table 1), a
3 consequence of prescribing the spatial dependency structure in the occurrence process.
4 Indeed, when re-doing the same experiments with multiple single-site WGs without inter-site
5 dependencies, only about 2% of all days are completely dry in the catchment and none of the
6 days are simulated as completely wet (Table 1). In a single-site WG setup, the chances for all
7 stations being dry or wet ultimately depend on the calibrated wet day frequencies at the eight
8 stations that remain below 0.5 in almost all months (see Figure 4). This implies that the
9 likelihood for dry conditions over the catchment is higher than for wet conditions.

10 Those days with complete dry or wet catchment conditions were further investigated in terms
11 of the temporal structure. Table 1 presents observed and multi-site simulated spell length
12 statistics for the catchment. In general, remarkably good agreement between observations and
13 the multi-site model is found. This is also true for longer spell lengths, where the spatio-
14 temporal correlation structure is only indirectly given as input to the WG. All of these results
15 imply that the calibrated multi-site WG not only captures the frequencies of spatially
16 aggregated binary series very well, it also does a surprisingly good job in reproducing multi-
17 day dry/wet spells of the *Thur* catchment.

18 4.2.2 Daily non-zero precipitation sums over the catchment

19 The above findings on the spatio-temporal correlation structure in the occurrence process also
20 give confidence that daily precipitation sums aggregated over the catchment are reasonably
21 simulated. To answer this user-relevant question, we first analyse seasonal distributions of
22 single-day precipitation area sums over the time-period 1961-2011 (Figure 7). Area sums are
23 defined as the precipitation sum over the eight stations. Note, that days with an area sum of
24 zero were excluded from this analysis and are not shown. The observations (grey boxplots)
25 show in the median only a weak inter-seasonal variability with somewhat higher sums during
26 summer. The spread in daily precipitation is smallest for winter and spring and largest for
27 summer owing to the higher extreme precipitation values observed. Common to all seasons is
28 a distribution that is heavily right-skewed ranging from nearly dry conditions up to about 220
29 mm day⁻¹. Note, that the spread shown here includes variability from year-to-year but also
30 within the season of the same year.

1 Compared to observations, the multi-site generator reproduces well the median of the
2 observed daily areal sums. The relative deviations remain rather small, ranging from -8.5% in
3 summer to +1.6% in autumn. Moreover, the multi-site model is able to capture about 95% of
4 the observed variability in the daily sums, while the single-site WG only explains about 13%.
5 Even for extreme areal precipitation, the deficiencies are rather small. Contrary to a multi-site
6 model, the areal sum derived from several single-site WGs over the catchment (red)
7 systematically underestimates median, variability and consequently the magnitude of extreme
8 precipitation amounts (Figure 7). The relative deviations from observations in the median
9 range from -28% in autumn to -18% in spring. The underestimation may be explained by the
10 fact that the single-site model rarely simulates days where all stations are wet (Sect. 4.2.1).
11 Also, the spatial structure of the precipitation amount is not accounted for.

12 4.2.3 Annual maximum precipitation sums of consecutive days over the catchment

13 The previous analysis has revealed a pronounced added value when incorporating spatial
14 dependencies in the stochastic simulation of daily areal precipitation sums over the *Thur*.

15 Similarly to Sect. 4.2.1, we want to go a step beyond and additionally include the temporal
16 structure. Note that by investigating spatial precipitation sums over multi-days, we explore the
17 limits of our WG. We analyse in Figure 8 annual maxima of observed (grey), and modelled
18 (blue and red for multi-site and single-site, respectively) precipitation sums over several
19 consecutive days (2, 5, and 10 days). This means that out of the aggregated catchment-time-
20 series we compute temporal sums over consecutive days and take the maximum in each year.

21 Regarding the performance of the calibrated WG in multi-site and single-site mode, Figure 8
22 shows that both are clearly underestimating the observed sums. Yet, the multi-site model
23 exhibits much smaller deviations from the observed distribution than the single-site model,
24 and hence the added value of the multi-site WG is clearly evident. In fact, the sums simulated
25 with the multi-site WG are larger by a factor of around 1.8 than those generated with the
26 single-site WG. Overall, deviations from observations are reduced from about -53% (single-
27 site WG) to about -17% (multi-site WG). The added value of the multi-site model is not
28 constant for different consecutive sums. Differences are larger at shorter multi-day sums and
29 decrease toward longer time-windows. This is related to the fact that the spatio-temporal
30 correlation structure at longer lags is not prescribed in the model as already seen in Sect. 4.2.1
31 and Table 1. The benefit of a multi-site WG in terms of maximum daily areal precipitation

1 sums is therefore restricted to consecutive sums over a few days only. And as a consequence
2 for time-windows of 30 days (or monthly sums), a single-site WG performs equally good as a
3 multi-site WG (not shown), as both models are calibrated for monthly sums at the eight
4 stations and consequently at the catchment.

5 **5 Discussion**

6 The incorporation of inter-station dependencies in the stochastic model brings substantial
7 added value over multiple single-site models regarding daily and multi-day areal precipitation
8 sums over the *Thur* catchment. Similar benefits from the multi-site WG would be expected
9 for other Alpine catchments and regions with complex topography, where correlations
10 between sites are significant but well below unity. For very homogeneous regimes (inter-
11 station correlation near unity) one single-site WG would be sufficient for the catchment-area,
12 whereas for low spatial correlations several independent single-site WGs can be used.

13 A stochastic simulation with multi-site correlation structure comes with additional uncertainty
14 from parameter estimations, additional implementation complexity and additional
15 computational costs. The decision for incorporating spatial dependencies must therefore be
16 balanced with the benefit. A careful inspection of the observed precipitation regime and its
17 spatial structure over the catchment prior to the simulation is necessary to decide in favour or
18 against multi-site simulation. This is also important in terms of validation: for a large
19 catchment area that is frequently affected by frontal passages, the validation of the
20 precipitation generator should include more complex space-time dependency analyses. An
21 example is the probability of a certain precipitation amount at a particular station given
22 precipitation at a neighbouring station some days earlier.

23 In the following, we want to elaborate more on the question, why we have implemented the
24 rather simple multi-site precipitation model of Wilks (1998) and not a more sophisticated one.
25 As already mentioned in the introduction, one premise of our work was to implement a
26 stochastic tool that can be subsequently applied in a climate change context. This means that
27 the number of model parameters needs to be kept limited for practical purposes such as
28 calibration handling and evaluation of parameter changes from multi-models. An approach,
29 such as NHMM is conditioned on atmospheric circulation, changes of which would need to
30 be constrained when used as a downscaling technique. However, from model evaluation
31 studies it is well-known that climate models are prone to substantial circulation errors (e.g.

1 van Haren et al., 2012; van Ulden and van Oldenborgh, 2006) with effects on the local
2 precipitation. Furthermore, the overall performance of a NHMM is highly dependent on the
3 predictive power of atmospheric circulation patterns and the number of synoptic weather
4 states, respectively (Schiemann and Frei, 2010). In winter, we would expect a NHMM to
5 perform better than in summer, when precipitation process is mainly dominated by local-scale
6 convective processes triggered by orography. However, we need a downscaling technique that
7 equally applies to all seasons. Also, for a small catchment scale such as the Thur , the
8 variability of the local precipitation pattern is pre-dominantly caused by physiographic
9 factors, such as height differences, or shielding effects, rather than by large-scale atmospheric
10 patterns. As was shown in Table 1, at around 70% of all days over 1961-2011 all stations in
11 the catchment are simultaneously dry or wet. Under these circumstances the use of a NHMM
12 would be feasible after careful calibration. For all these reasons, the precipitation generator by
13 Wilks (1998) is in our view the more direct approach to guarantee the spatial consistency for
14 the stations in our catchment.

15 For many impact applications gridded precipitation data instead of multiple scattered stations
16 would be beneficial. This demand could be achieved by interpolating the spatially consistent
17 synthetic station data over the area of interest. A more sophisticated and elegant method,
18 however, is to build a field generator, for instance by high-dimensional random Gaussian
19 fields (e.g. Pegram and Clothier, 2001), random cascade models (e.g. Over and Gupta, 1996)
20 or Poisson cluster models (e.g. Burton et al., 2008). An alternative would be to rely on
21 geostatistical methods, for instance by prescribing a spatial correlation function at gauged and
22 ungauged locations, that additionally requires specifying also parameters of the WG between
23 the sites (e.g. Wilks, 2009). In regions with complex topography this additional interpolation
24 is not straightforward. It could be alleviated by explicitly including information of
25 topographic aspects (e.g. altitude, aspect and slope) in a GLM- (McCullagh and Nelder, 1989)
26 or Bayesian Hierarchical modelling-approach (Gelman and Hill, 2006). These are appealing
27 frameworks that allow the modelling of physiographic dependencies in the precipitation
28 amount and occurrence model. However, this alone is not sufficient for a space-time weather
29 generator as the spatial dependence of daily precipitation is also determined by spatial
30 autocorrelation and not just the physiographic conditioning of parameters. Clearly, the
31 development of a gridded space-time weather generator dealing with spatial autocorrelation,
32 physiographic conditioning, intermittence and temporal autocorrelation is highly challenging
33 and needs fundamental methodological development. This is beyond the scope in the present

1 study, where our main focus was to develop an easy-to-use statistical downscaling tool for
2 current and future climate.

3 **6 Summary and Outlook**

4 The multi-site precipitation generator of Wilks (1998) has been successfully developed,
5 implemented and tested over the Swiss alpine river catchment *Thur*. The precipitation
6 generator treats precipitation occurrence as a Markov chain and simulates non-zero daily
7 precipitation amounts from a mixture model of two exponential distributions. The spatial
8 dependency is ensured by running the WG with spatially correlated random numbers. The
9 model was calibrated on a monthly basis by using daily station data over a 51-year long time-
10 period from 1961-2011, and extensively compared to the observed record and to simulations
11 based on multiple independent single-site WGs.

12 Our main findings of this study are:

- 13 • The multi-site precipitation generator realistically reproduces key precipitation
14 statistics at single stations, including the annual cycle, quantiles of non-zero
15 precipitation amounts, multi-day spells and multi-day amount statistics.
- 16 • The precipitation generator is able to generate relatively large stochastic variability.
17 Nevertheless, it is rather low compared to observed inter-annual variability where it
18 underestimates inter-annual variability by a factor of 3.
- 19 • The incorporation of inter-station dependencies in the stochastic process brings
20 substantial added value over multiple single-site WGs. The median of daily area sums
21 are higher by about a factor of 1.3 than those from independent single-site models. In
22 addition, the multi-site WG is able to capture about 95% of the observed variability,
23 while the single-site WG only explains about 13%. Annual maxima of multi-day sums
24 over the catchment increase by about a factor of 1.8 by incorporating the inter-site
25 dependence in the stochastic simulations.
- 26 • The added value is largest when the precipitation regime is subject to a large spatial
27 and temporal heterogeneity as it is the case over the *Thur* catchment.

28 These results provide confidence that the developed precipitation generator is a helpful tool to
29 realistically simulate mean aspects of the current climate. We therefore conclude that this
30 generator can subsequently be used as a statistical downscaling tool to generate synthetic

1 time-series consistent with mean aspects of the future climate. Although there is substantial
2 improvement compared to a simple delta-change approach, from an end-user perspective
3 some relevant limitations need to be kept in mind: The synthetically generated time-series (for
4 current or future climate) do not fully capture the day-to-day and multi-day variability of
5 precipitation. Extreme values and longer spell lengths are hence underestimated. The
6 generator further underestimates the year-to-year variability in monthly precipitation sums.
7 Therefore, care should be taken when using the precipitation generator as a tool for a broad
8 risk assessment, in particular with respect to extreme events.

9 These inherent limitations point to potential future refinements of the presented model: (a) To
10 better reproduce extreme precipitation, we intend to implement a three-state Markov chain
11 model with the states dry, wet, and very wet and with state-dependent PDFs. From this, we
12 expect a substantial improvement of one-day and multi-day extremes as well as a better
13 reproduction of multi-day precipitation sums. (b) To alleviate the underestimation of inter-
14 annual variability, we will introduce a non-stationary model. This could be accomplished by
15 sampling from a distribution of observed WG parameters (instead of taking the mean) or by
16 formulating a regression model using large-scale atmospheric variables as predictors (see e.g.
17 Furrer and Katz, 2007).

18 Beside these methodological improvements the precipitation generator will be subject to two
19 extensions: (a) the coupling of daily minimum and maximum temperature as additional
20 atmospheric variables and (b) the adjustment of the WG parameters to represent a future mean
21 climate. Finally, the time-series over the Thur catchment will serve as input for a hydrological
22 model to assess the added value of multi- versus single-site WGs in terms of runoff and to
23 assess the implications of the systematic biases of the WG for hydrological quantities.

24

1 **Acknowledgements**

2 This work is supported by the ETH Research Grant CH2-01 11-1. We would like to thank the
3 Center for Climate Systems Modeling (C2SM) at ETH Zurich for providing technical and
4 scientific support.

5

1 **References**

- 2 Akaike, H.: A new look at the statistical model identification, *IEEE Trans. Automat. Contr.*,
3 19(6), 716–723, doi:10.1109/TAC.1974.1100705, 1974.
- 4 Allen, M. R. and Ingram, W. J.: Constraints on future changes in climate and the hydrologic
5 cycle., *Nature*, 419(6903), 224–32, doi:10.1038/nature01092, 2002.
- 6 BAFU: Hydrologischer Atlas der Schweiz HADES, *Hydrol. Atlas der Schweiz HADES*
7 [online] Available from: <http://www.hydrologie.unibe.ch/hades/index.html> (Accessed 10
8 April 2014), 2007.
- 9 BAFU: Auswirkungen der Klimaänderung auf Wasserressourcen und Gewässer.
10 Synthesebericht zum Projekt «Klimaänderung und Hydrologie in der Schweiz» (CCHydro),
11 Bern, Switzerland., 2012.
- 12 Baigorria, G. A. and Jones, J. W.: GiST: A Stochastic Model for Generating Spatially and
13 Temporally Correlated Daily Rainfall Data, *J. Clim.*, 23(22), 5990–6008,
14 doi:10.1175/2010JCLI3537.1, 2010.
- 15 Bárdossy, A. and Pegram, G.: Copula based multisite model for daily precipitation
16 simulation, *Hydrol. Earth Syst. Sci. Discuss.*, 6(3), 4485–4534, doi:10.5194/hessd-6-4485-
17 2009, 2009.
- 18 Begert, M., Seiz, G., Schlegel, T., Musa, M., Baudraz, G. and Moesch, M.: Homogenisierung
19 von Klimamessreihen der Schweiz und Bestimmung der Normwerte 1961-1990, Zurich.,
20 2003.
- 21 Bellone, E., Hughes, J. and Guttorp, P.: A hidden Markov model for downscaling synoptic
22 atmospheric patterns to precipitation amounts, *Clim. Res.*, 15, 1–12, doi:10.3354/cr015001,
23 2000.
- 24 Bosshard, T., Kotlarski, S., Ewen, T. and Schär, C.: Spectral representation of the annual
25 cycle in the climate change signal, *Hydrol. Earth Syst. Sci.*, 15(9), 2777–2788,
26 doi:10.5194/hess-15-2777-2011, 2011.

- 1 Boughton, W. C.: A daily rainfall generating model for water yield and flood studies, Monash
2 Univ., Melbourne, Victoria, Australia., 1999.
- 3 Buishand, T. A. and Brandsma, T.: Multisite simulation of daily precipitation and temperature
4 in the Rhine Basin by nearest-neighbor resampling, *Water Resour. Res.*, 37(11), 2761–2776,
5 doi:10.1029/2001WR000291, 2001.
- 6 Burden, R. and Faires, J. D.: *Numerical Analysis*, 9th Ed., edited by Michelle Julet., 2010.
- 7 Burton, A., Kilsby, C. G., Fowler, H. J., Cowpertwait, P. S. P. and O’Connell, P. E.: RainSim:
8 A spatial–temporal stochastic rainfall modelling system, *Environ. Model. Softw.*, 23(12),
9 1356–1369, doi:10.1016/j.envsoft.2008.04.003, 2008.
- 10 Calanca, P.: Climate change and drought occurrence in the Alpine region: How severe are
11 becoming the extremes?, *Glob. Planet. Change*, 57(1-2), 151–160,
12 doi:10.1016/j.gloplacha.2006.11.001, 2007.
- 13 CH2014-Impacts: Toward quantitative scenario of climate change impacts in Switzerland,
14 published by: OCCR, FOEN, MeteoSwiss, C2SM, Agroscope, and ProClim, Bern,
15 Switzerland., 2014.
- 16 Chandler, R. E.: Rglimclim, [online] Available from:
17 <http://www.homepages.ucl.ac.uk/~ucakarc/work/glimclim.html> (Accessed 10 April 2014),
18 2014.
- 19 Chandler, R. E. and Wheater, H. S.: Analysis of rainfall variability using generalized linear
20 models: A case study from the west of Ireland, *Water Resour. Res.*, 38(10), 1192,
21 doi:10.1029/2001WR000906, 2002.
- 22 Cowpertwait, P. S. P.: A Generalized Spatial-Temporal Model of Rainfall Based on a
23 Clustered Point Process, *Proc. R. Soc. A Math. Phys. Eng. Sci.*, 450(1938), 163–175,
24 doi:10.1098/rspa.1995.0077, 1995.
- 25 Fatichi, S., Ivanov, V. Y. and Caporali, E.: Simulation of future climate scenarios with a
26 weather generator, *Adv. Water Resour.*, 34(4), 448–467,
27 doi:10.1016/j.advwatres.2010.12.013, 2011.

- 1 Frei, C. and Schär, C.: A precipitation climatology of the Alps from high-resolution rain-
2 gauge observations, *Int. J. Climatol.*, 18(8), 873–900, doi:10.1002/(SICI)1097-
3 0088(19980630)18:8<873::AID-JOC255>3.0.CO;2-9, 1998.
- 4 Fundel, F., Jörg-Hess, S. and Zappa, M.: Monthly hydrometeorological ensemble prediction
5 of streamflow droughts and corresponding drought indices, *Hydrol. Earth Syst. Sci.*, 17(1),
6 395–407, doi:10.5194/hess-17-395-2013, 2013.
- 7 Furrer, E. M. and Katz, R. W.: Generalized linear modeling approach to stochastic weather
8 generators, *Clim. Res.*, 34, 129–144, doi:10.3354/cr034129, 2007.
- 9 Gabriel, K. R. R. and Neumann, Y.: A Markov chain model for daily rainfall occurrence at
10 Tel Aviv, *Quart. J. Roy. Meteorol. Soc.*, 88, 90–95, 1962.
- 11 Gelman, A. and Hill, J.: *Data Analysis Using Regression and Multilevel/Hierarchical Models*,
12 Cambridge University Press., 2006.
- 13 Gregory, J. ., Wigley, T. M. . and Jones, P. .: Application of Markov models to area-average
14 daily precipitation series and interannual variability in seasonal totals., *Clim. Dyn.*, 8, 299–
15 310, doi:10.1007/BF00209669, 1993.
- 16 Van Haren, R., van Oldenborgh, G. J., Lenderink, G., Collins, M. and Hazeleger, W.: SST
17 and circulation trend biases cause an underestimation of European precipitation trends, *Clim.*
18 *Dyn.*, 40(1-2), 1–20, doi:10.1007/s00382-012-1401-5, 2012.
- 19 Held, I. M. and Soden, B. J.: Robust Responses of the Hydrological Cycle to Global
20 Warming, *J. Clim.*, 19(21), 5686–5699, doi:10.1175/JCLI3990.1, 2006.
- 21 Hertig, E. and Jacobeit, J.: A novel approach to statistical downscaling considering
22 nonstationarities: application to daily precipitation in the Mediterranean area, *J. Geophys.*
23 *Res. Atmos.*, 118(2), 520–533, doi:10.1002/jgrd.50112, 2013.
- 24 Higham, N. J.: Matrix nearness problems and applications, in *Applications of Matrix Theory*,
25 edited by M. Gover and S. Barnett, pp. 1–27, Oxford University Press., 1989.

- 1 Higham, N. J.: Cholesky factorization, *Wiley Interdiscip. Rev. Comput. Stat.*, 1(2), 251–254,
2 doi:10.1002/wics.18, 2009.
- 3 Hughes, J. P., Guttorp, P. and Charles, S. P.: A non-homogeneous hidden Markov model for
4 precipitation occurrence, *J. R. Stat. Soc. Ser. C (Applied Stat.)*, 48(1), 15–30,
5 doi:10.1111/1467-9876.00136, 1999.
- 6 Hurrell, J. W., Kushnir, Y., Ottersen, G. and Visbeck, M.: *The North Atlantic Oscillation:
7 Climatic Significance and Environmental Impact*, edited by J. W. Hurrell, Y. Kushnir, G.
8 Ottersen, and M. Visbeck, American Geophysical Union, Washington, D. C., 2003.
- 9 Huser, R. and Davison, A. C.: Space-time modelling of extreme events, *J. R. Stat. Soc. Ser. B
10 (Statistical Methodol.)*, 76(2), 439–461, doi:10.1111/rssb.12035, 2014.
- 11 Isotta, F. A., Frei, C., Weilguni, V., Perčec Tadić, M., Lassègues, P., Rudolf, B., Pavan, V.,
12 Cacciamani, C., Antolini, G., Ratto, S. M., Munari, M., Micheletti, S., Bonati, V., Lussana,
13 C., Ronchi, C., Panettieri, E., Marigo, G. and Vertačnik, G.: The climate of daily precipitation
14 in the Alps: development and analysis of a high-resolution grid dataset from pan-Alpine rain-
15 gauge data, *Int. J. Climatol.*, 34, 1657–1675, doi:10.1002/joc.3794, 2013.
- 16 Jasper, K., Calanca, P., Gyalistras, D. and Fuhrer, J.: Differential impacts of climate change
17 on the hydrology of two alpine river basins, *Clim. Res.*, 26, 113–129, 2004.
- 18 Kioutsioukis, I., Melas, D. and Zanis, P.: Statistical downscaling of daily precipitation over
19 Greece, *Int. J. Climatol.*, 28, 679–691, doi:10.1002/joc, 2008.
- 20 Köplin, N., Viviroli, D., Schädler, B., Weingartner, R. and Bormann, H.: How does climate
21 change affect mesoscale catchments in Switzerland? a framework for a comprehensive
22 assessment., *Adv. Geosci.*, 27, 111–119, doi:10.5194/adgeo-27-111-2010, 2010.
- 23 Kunstmann, H., Krause, J. and Mayr, S.: Inverse distributed hydrological modelling of Alpine
24 catchments, *Hydrol. Earth Syst. Sci.*, 10, 395–412, 2006.
- 25 Maraun, D., Wetterhall, F., Ireson, A. M., Chandler, R. E., Kendon, E. J., Widmann, M.,
26 Brien, S., Rust, H. W., Sauter, T., Themeßl, M. J., Venema, V. K. C., Chun, K. P.,
27 Goodess, C. M., Jones, R. G., Onof, C. J., Vrac, M. and Thiele-Eich, I.: Precipitation

1 downscaling under climate change: Recent developments to bridge the gap between
2 dynamical models and the end user, *Rev. Geophys.*, 48(3), RG3003,
3 doi:10.1029/2009RG000314, 2010.

4 McCullagh, P. and Nelder, J. A.: *Generalized linear models.*, Chapman and Hall, London
5 England., 1989.

6 Mehrotra, R., Srikanthan, R. and Sharma, A.: A comparison of three stochastic multi-site
7 precipitation occurrence generators, *J. Hydrol.*, 331(1-2), 280–292,
8 doi:10.1016/j.jhydrol.2006.05.016, 2006.

9 Mezghani, A. and Hingray, B.: A combined downscaling-disaggregation weather generator
10 for stochastic generation of multisite hourly weather variables over complex terrain:
11 Development and multi-scale validation for the Upper Rhone River basin, *J. Hydrol.*, 377,
12 245–260, doi:10.1016/j.jhydrol.2009.08.033, 2009.

13 Over, T. M. and Gupta, V. K.: A space-time theory of mesoscale rainfall using random
14 cascades, *J. Geophys. Res.*, 101(D21), doi:10.1029/96JD02033, 1996.

15 Paschalis, A., Molnar, P., Fatichi, S. and Burlando, P.: A stochastic model for high-resolution
16 space-time precipitation simulation, *Water Resour. Res.*, 49(12), 8400–8417,
17 doi:10.1002/2013WR014437, 2013.

18 Pegram, G. G. S. and Clothier, A. N.: High resolution space–time modelling of rainfall: the
19 “String of Beads” model, *J. Hydrol.*, 241(1-2), 26–41, doi:10.1016/S0022-1694(00)00373-5,
20 2001.

21 Peleg, N. and Morin, E.: Stochastic convective rain-field simulation using a high-resolution
22 synoptically conditioned weather generator (HiReS-WG), *Water Resour. Res.*, (50), 2124–
23 2139, doi:10.1002/2013WR014836, 2014.

24 Racsko, P., Szeidl, L. and Semenov, M. A.: A serial approach to local stochastic weather
25 models, *Ecol. Modell.*, 57(1-2), 27–41, doi:10.1016/0304-3800(91)90053-4, 1991.

26 Richardson, C. W.: Stochastic simulation of daily precipitation, temperature, and solar
27 radiation, *Water Resour. Res.*, 17(1), 182–190, doi:10.1029/WR017i001p00182, 1981.

- 1 Robertson, A., Kirshner, S. and Smyth, P.: Downscaling of daily rainfall occurrence over
2 northeast Brazil using a hidden Markov model, *J. Clim.*, 17, 4407–4424 [online] Available
3 from: <http://journals.ametsoc.org/doi/abs/10.1175/jcli-3216.1> (Accessed 9 February 2015),
4 2004.
- 5 Robertson, A., Moron, V. and Swarinoto, Y.: Seasonal predictability of daily rainfall statistics
6 over Indramayu district, Indonesia, *Int. J. Climatol.*, 29, 1449–1462, doi:10.1002/joc, 2009.
- 7 Samuels, R., Rimmer, A. and Alpert, P.: Effect of extreme rainfall events on the water
8 resources of the Jordan River, *J. Hydrol.*, 375(3-4), 513–523,
9 doi:10.1016/j.jhydrol.2009.07.001, 2009.
- 10 Schiemann, R. and Frei, C.: How to quantify the resolution of surface climate by circulation
11 types: An example for Alpine precipitation, *Phys. Chem. Earth, Parts A/B/C*, 35(9-12), 403–
12 410, doi:10.1016/j.pce.2009.09.005, 2010.
- 13 Schwarz, G.: Estimating the Dimension of a Model, *Ann. Stat.*, 6(2), 461–464,
14 doi:10.1214/aos/1176344136, 1978.
- 15 Tallis, G. M. and Light, R.: The Use of Fractional Moments for Estimating the Parameters of
16 a Mixed Exponential Distribution, *Technometrics*, 10(1), 161–175,
17 doi:10.1080/00401706.1968.10490543, 1968.
- 18 Themeßl, J. M., Gobiet, A. and Leuprecht, A.: Empirical-statistical downscaling and error
19 correction of daily precipitation from regional climate models, *Int. J. Climatol.*, 31(10), 1530–
20 1544, doi:10.1002/joc.2168, 2011.
- 21 Van Ulden, A. P. and van Oldenborgh, G. J.: Large-scale atmospheric circulation biases and
22 changes in global climate model simulations and their importance for climate change in
23 Central Europe, *Atmos. Chem. Phys.*, 6(4), 863–881, doi:10.5194/acp-6-863-2006, 2006.
- 24 Vrac, M. and Naveau, P.: Stochastic downscaling of precipitation: From dry events to heavy
25 rainfalls, *Water Resour. Res.*, 43(7), W07402, doi:10.1029/2006WR005308, 2007.

- 1 Wheater, H. S., Chandler, R. E., Onof, C. J., Isham, V. S., Bellone, E., Yang, C., Lekkas, D.,
2 Lourmas, G. and Segond, M.-L.: Spatial-temporal rainfall modelling for flood risk estimation,
3 Stoch. Environ. Res. Risk Assess., 19(6), 403–416, doi:10.1007/s00477-005-0011-8, 2005.
- 4 Wilks, D. S.: Multisite generalization of a daily stochastic precipitation generation model, J.
5 Hydrol., 210(1-4), 178–191, doi:10.1016/S0022-1694(98)00186-3, 1998.
- 6 Wilks, D. S.: Interannual variability and extreme-value characteristics of several stochastic
7 daily precipitation models, Agric. For. Meteorol., 93(3), 153–169, doi:10.1016/S0168-
8 1923(98)00125-7, 1999a.
- 9 Wilks, D. S.: Simultaneous stochastic simulation of daily precipitation, temperature and solar
10 radiation at multiple sites in complex terrain, Agric. For. Meteorol., 96(1-3), 85–101,
11 doi:10.1016/S0168-1923(99)00037-4, 1999b.
- 12 Wilks, D. S.: A gridded multisite weather generator and synchronization to observed weather
13 data, Water Resour. Res., 45(10), n/a–n/a, doi:10.1029/2009WR007902, 2009.
- 14 Wilks, D. S.: Statistical Methods in the Atmospheric Sciences, Academic Press., 2011.
- 15 Wilks, D. S. and Wilby, R. L.: The weather generation game: a review of stochastic weather
16 models, Prog. Phys. Geogr., 23(3), 329–357, doi:10.1177/030913339902300302, 1999.
- 17 Yang, C., Chandler, R. E., Isham, V. S. and Wheeler, H. S.: Spatial-temporal rainfall
18 simulation using generalized linear models, Water Resour. Res., 41(11), W11415,
19 doi:10.1029/2004WR003739, 2005.

20

21

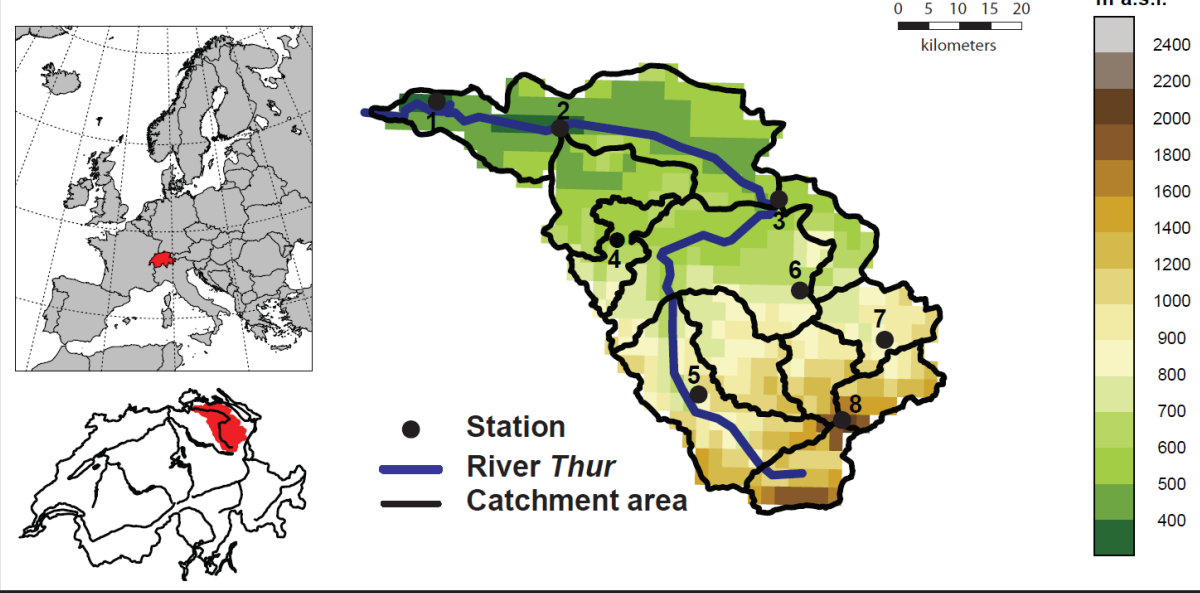
1 Table 1. Frequencies (given in percent) of a completely wet or dry catchment together with
 2 the frequencies of its spell lengths. The observed (OBS) frequencies are calculated over 1961-
 3 2011. The multi-site simulated frequencies are given by the mean of 100 runs over 51 years
 4 (1961-2011).

		Wet catchment			Dry catchment		
		<i>OBS</i>	<i>multi-site</i>	<i>single-site</i>	<i>OBS</i>	<i>multi-site</i>	<i>single-site</i>
Overall	frequency	25	25	0	45	44	2
Frequencies of spell lengths	1	34.8	34.4	0.0	14.1	17.3	2
	2	27.3	29.4	0.0	16.2	20.7	0.0
	3	16.7	18.2	0.0	13.0	18.2	0.0
	4	11.5	9.7	0.0	10.8	14.1	0.0
	5	4.1	4.7	0.0	9.1	10.3	0.0
	6	2.7	2.1	0.0	5.9	7.0	0.0
	7	0.9	0.9	0.0	7.2	4.7	0.0
	8	0.7	0.4	0.0	5.1	3.0	0.0
	9	0.6	0.2	0.0	3.5	1.9	0.0
	10	0.2	0.0	0.0	3.5	1.2	0.0

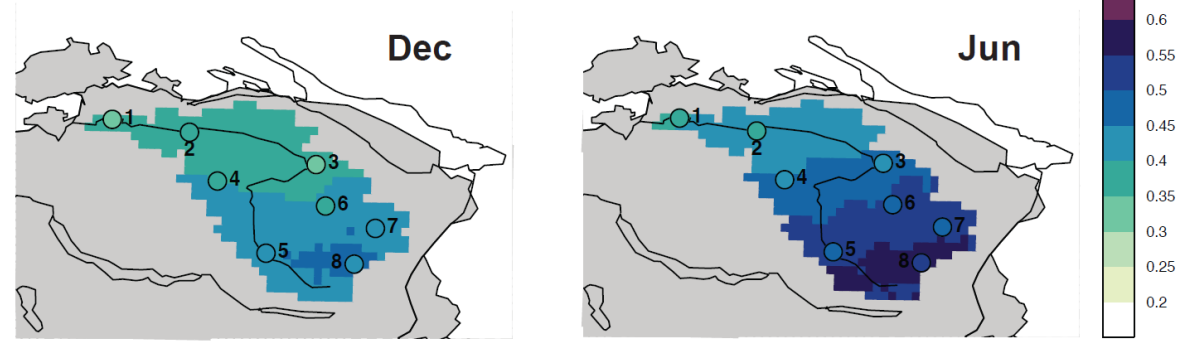
5

6

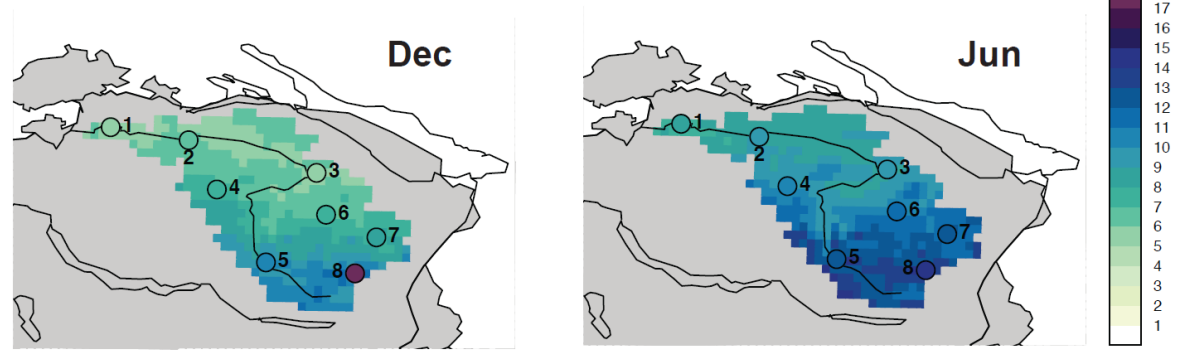
a) Location and topography of catchment



b) Wet day frequency



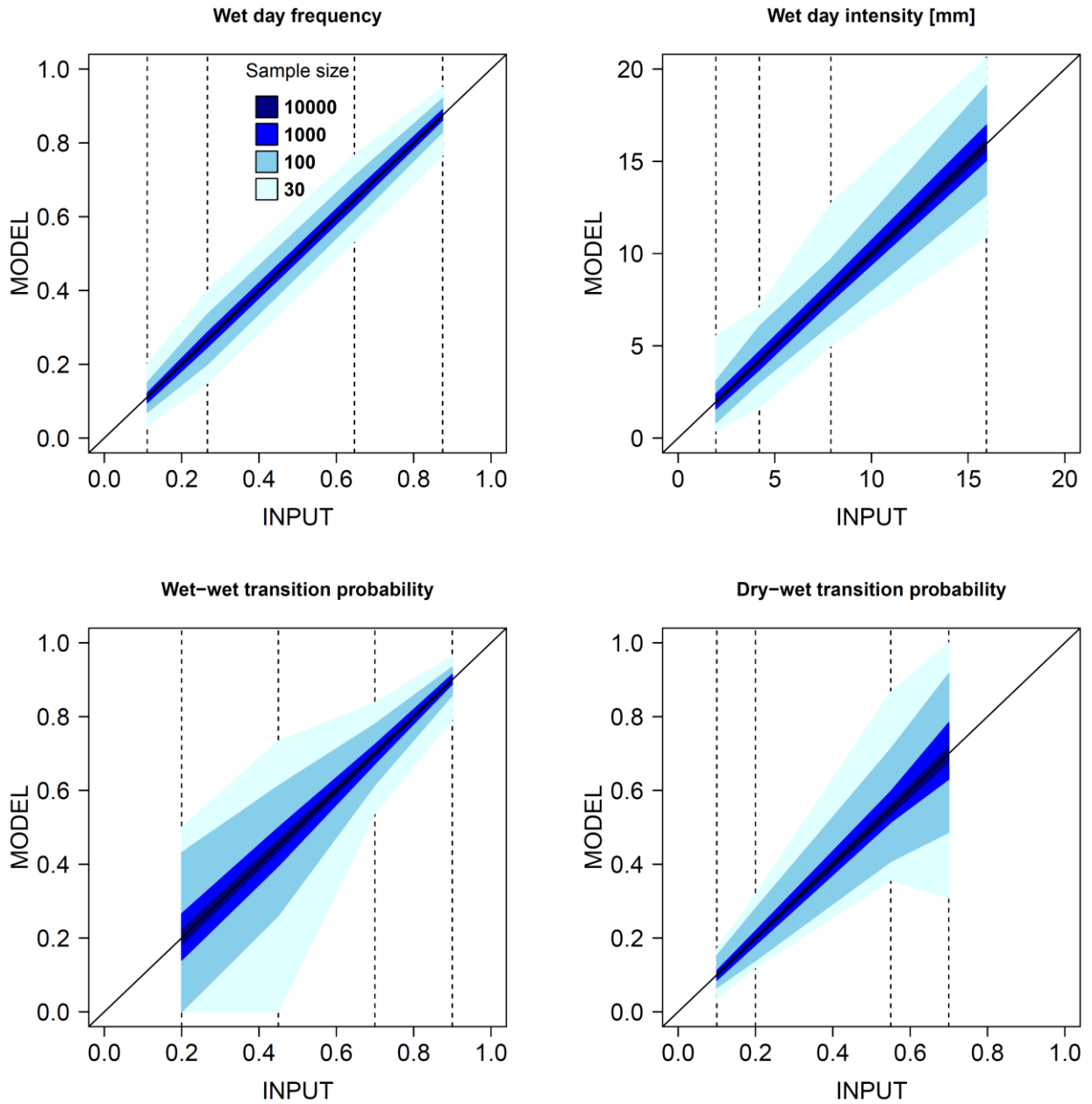
c) Wet day intensity [mm/d]



1
2
3
4
5

Figure 1. a) The catchment of the river *Thur*, located in north-eastern Switzerland, together with the underlying topography (in m.a.s.l.). The dots indicate the locations of the investigated stations. 1: *Andelfingen* (AFI, 47.60°N / 8.69°E), 2: *Frauenfeld* (FRF, 47.57°N /

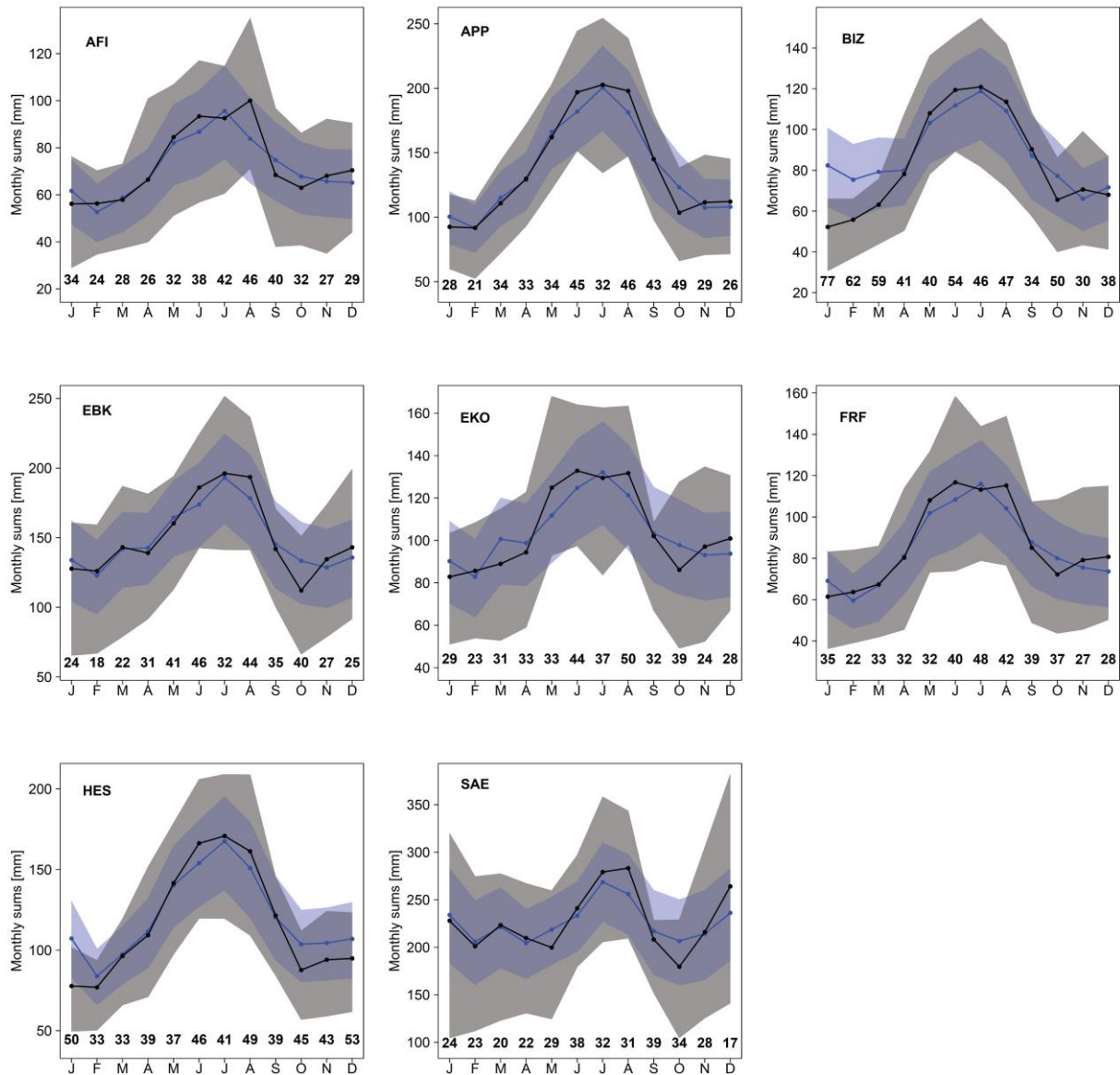
1 8.89°E), 3: *Bischofszell* (BIZ, 47.50°N / 9.23°E), 4: *Eschlikon* (EKO, 47.45°N / 8.97°E), 5:
2 *Ebnat-Kappel* (EBK, 47.27°N / 9.11°E), 6: *Herisau* (HES, 47.39°N / 9.26°E), 7: *Appenzell*
3 (*APP*, 47.34°N / 9.40°E), 8: *Saentis* (SAE, 47.25°N / 9.34°E). The polygons represent sub-
4 catchments. b) Observed precipitation climatology of the wet day frequency (1961-2011)
5 derived from a 2.2km x 2.2km gridded daily precipitation dataset (Frei and Schär, 1998) for
6 December and June. The grey polygons represent the north-eastern part of the Swiss territory.
7 c) The same as in b), but for wet day intensity (in mm day⁻¹). A wet day is defined as a day
8 with precipitation amount equal or higher than 1mm day⁻¹. The filled circle symbols point to
9 the station locations (as in a) together with the observed station measurements.
10



1

2 Figure 2. Reproduction of average wet day frequency (wdf), mean wet day intensity (wdi),
 3 wet-wet transition probability (p_{11}) and dry-wet transition probability (p_{01}) for the four
 4 idealized climate regime ranging from very dry (left) to very wet (right) as indicated by
 5 dashed lines. The shaded areas correspond to the range between the 2.5% and the 97.5%
 6 empirical quantiles of 100 realizations. Results are shown for sample sizes of 10,000, 1000,
 7 100 and 30 (grey shading).

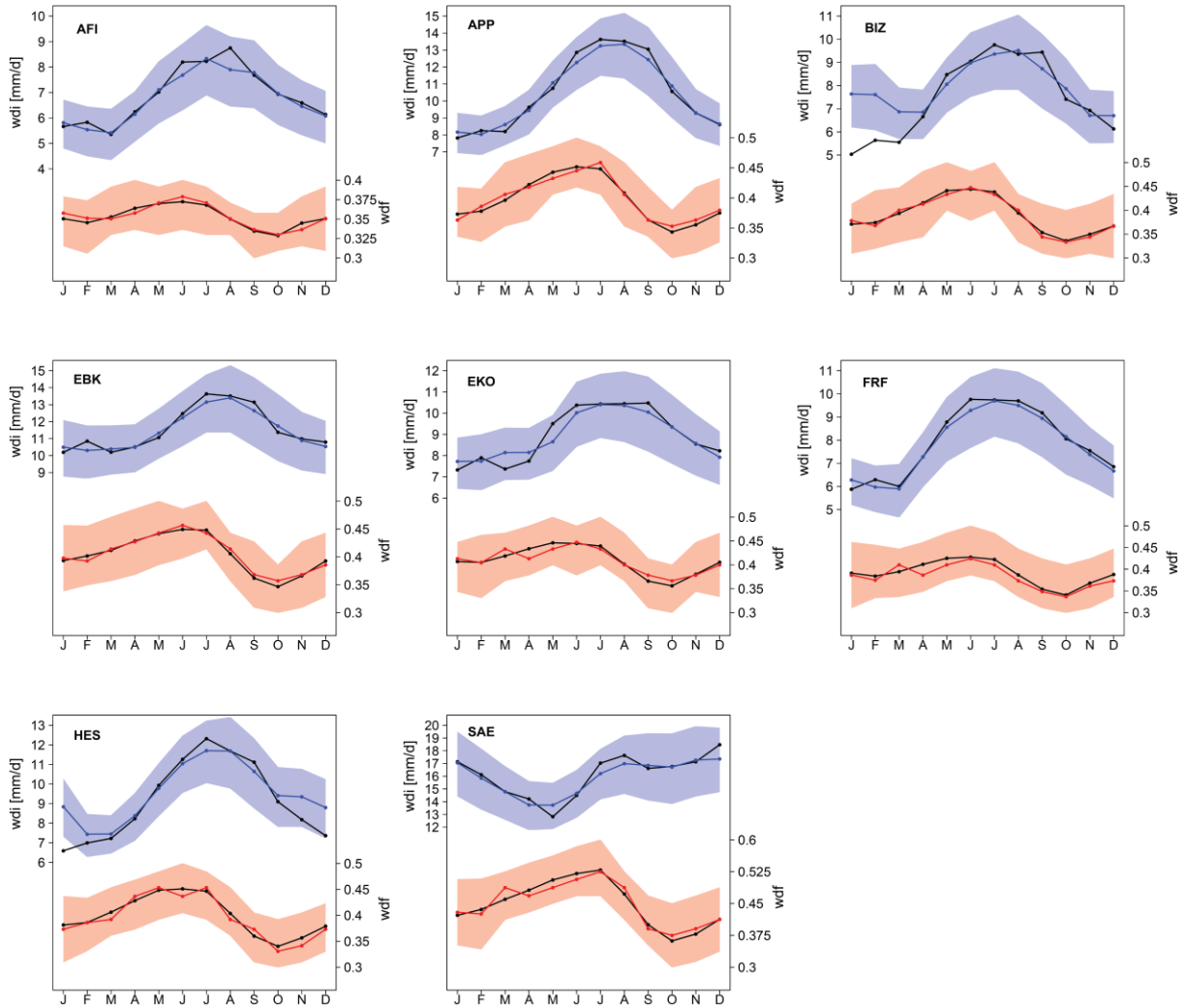
8



1

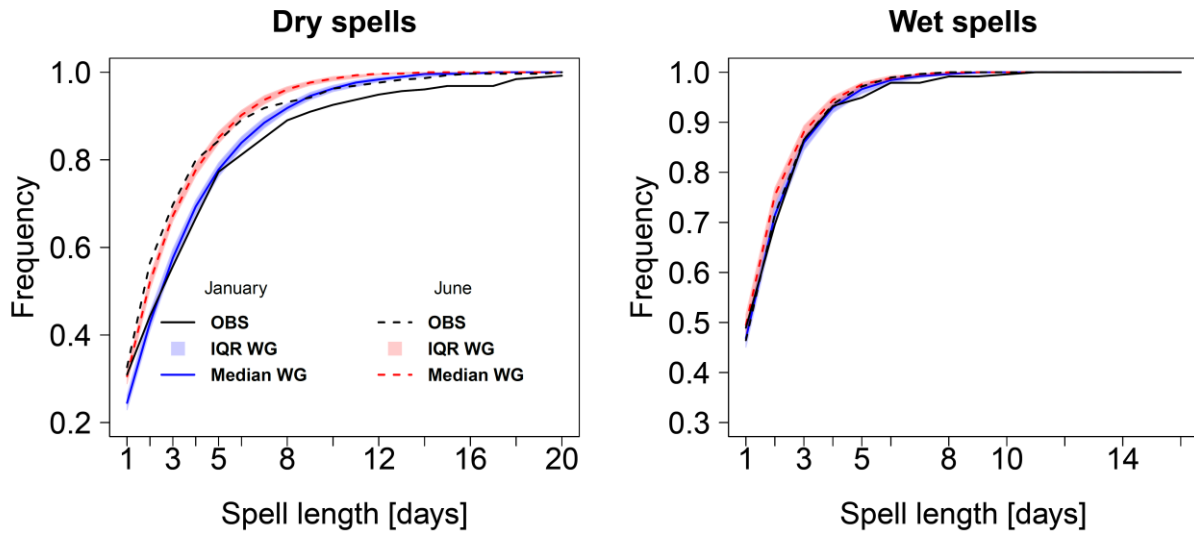
2 Figure 3. Long-term mean and variability of monthly precipitation sums during the period
 3 1961-2011 for eight stations in the *Thur* catchment. The black (blue) lines refer to the mean
 4 annual cycle of observed (modelled) precipitation sums. The grey (blue) shaded areas
 5 represent the inter-quartile ranges of observed (simulated) monthly precipitation sums. The
 6 simulation comprises 100 realizations covering each 51 years. The numbers at the bottom
 7 indicate for each month the percentage of variance explained by the precipitation generator.
 8 Note that the scale of the y-axis differ between different stations.

9

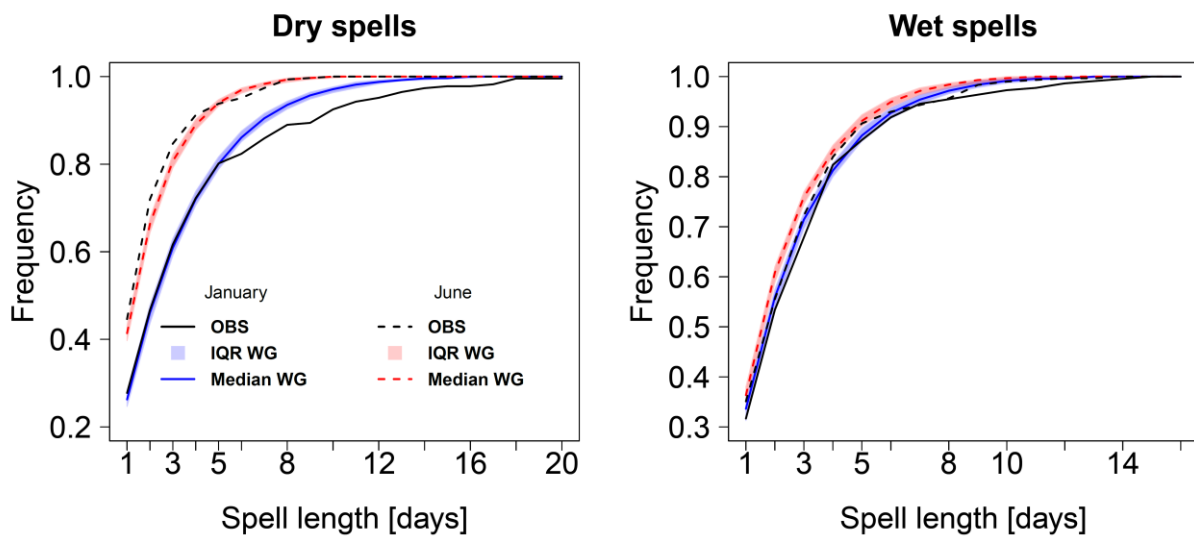


1
 2 Figure 4. Observed and modelled monthly mean wet day intensity (blue) and frequency (red)
 3 at eight stations during 1961-2011. The black (coloured) lines indicate the observed
 4 (modelled) values. The blue (red) shaded areas correspond to the inter-quartile range across
 5 the set of synthetic daily time-series. They comprise 100 runs covering each 51 years.
 6

Andelfingen (AFI)

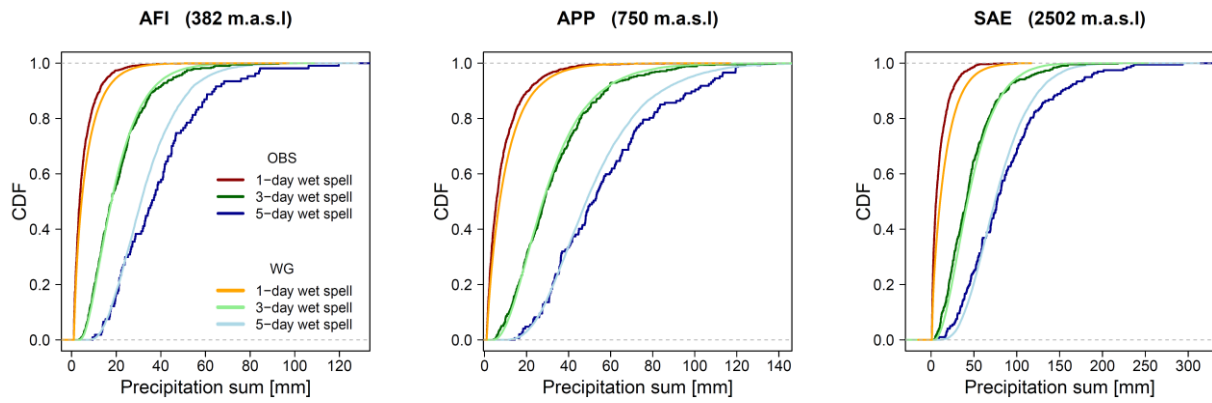


Saentis (SAE)

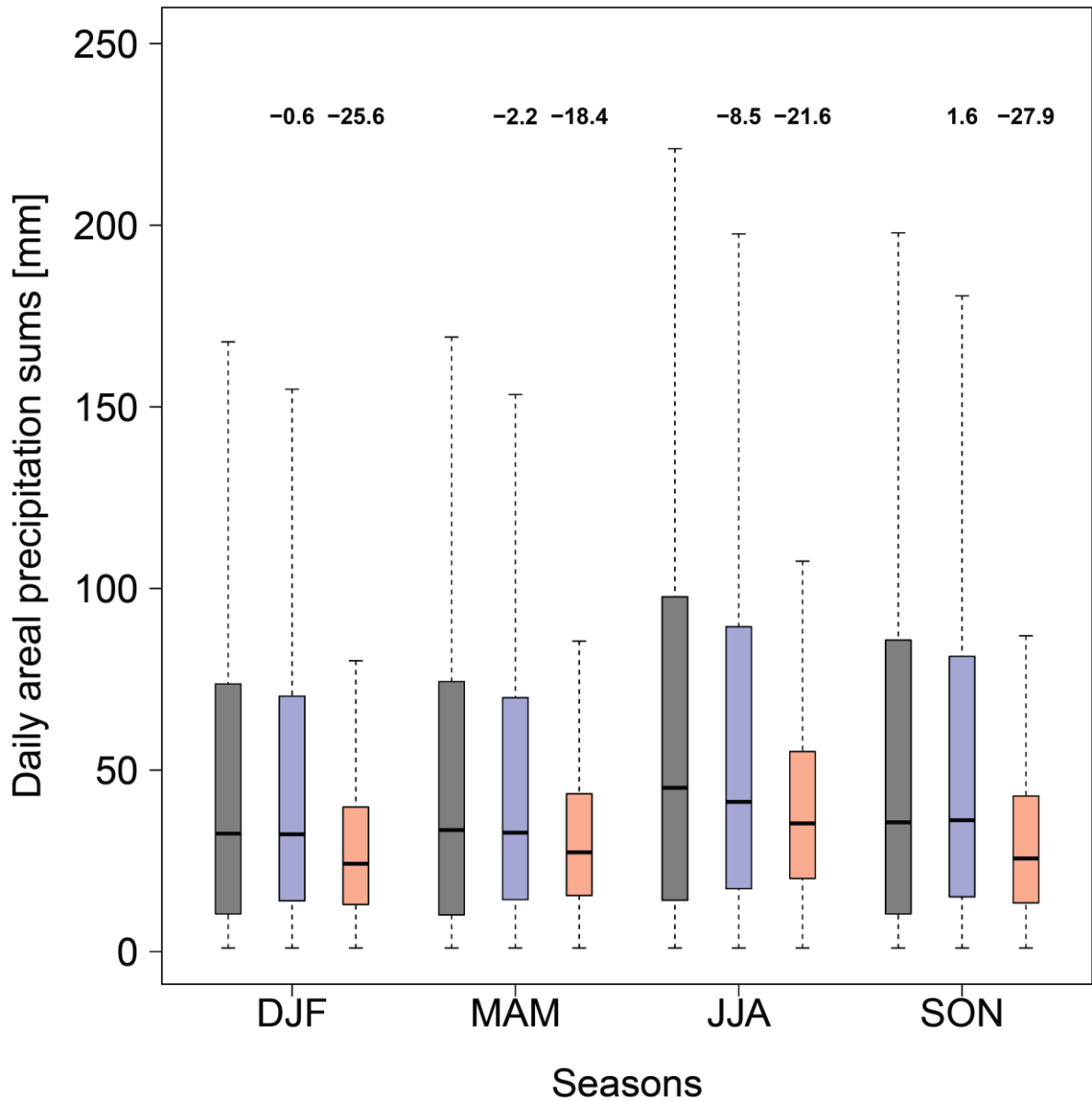


1
2
3
4
5
6
7

Figure 5. Cumulative distribution of the observed and simulated dry (left) and wet (right) spell length frequencies for the lowland station *Andelfingen* (top) and the mountain station *Saentis* (bottom). Results are for January and June during the time period of 1961-2011. The coloured area (line) represents the inter-quartile range (median) of the 100 realizations covering each 51 year-long daily time-series.

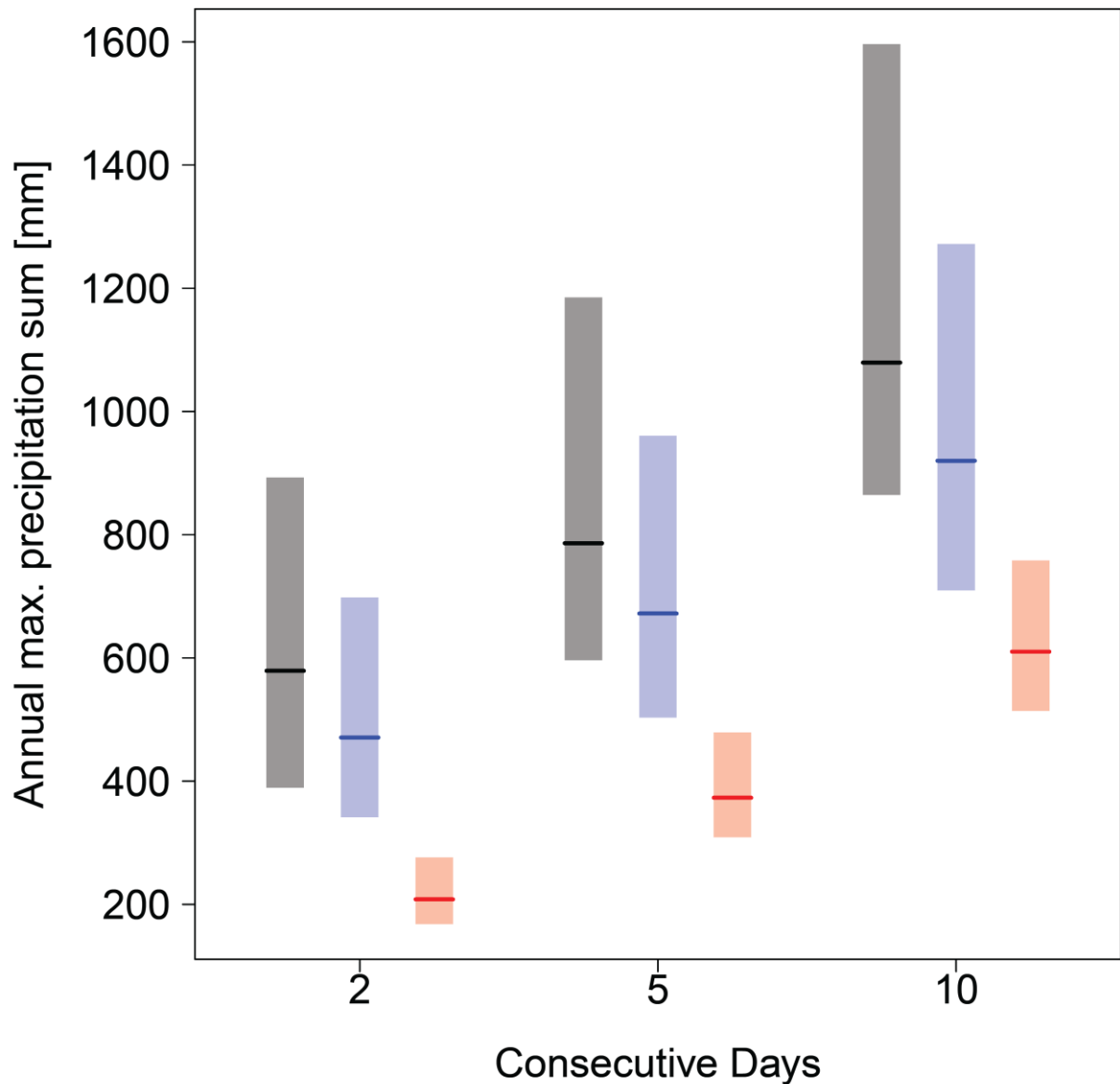


1
2 Figure 6. Cumulative distribution functions (CDFs) of multi-day precipitation sums for the
3 three stations *Andelfingen* (AFI), *Appenzell* (APP) and *Saentis* (SAE). The lines represent the
4 CDFs of non-zero precipitation amounts over one day (red), over three consecutive wet days
5 (green) and over five consecutive wet days (blue). Darker and lighter colours refer to
6 observations and simulations, respectively. The observed CDFs have been derived from a 51-
7 year long daily time-series between 1961 and 2011, those of the weather generator from 100
8 realizations of 51-year long daily simulations. Note that the scaling of the horizontal axis
9 differs between different stations.
10



1
2
3
4
5
6
7
8
9

Figure 7. Daily non-zero precipitation sums over the catchment for the four seasons during 1961-2011. Daily Precipitation intensity of the eight stations are summed and days with an area sum of zero are excluded. Boxplots of observed daily sums (grey), of multi-site simulated time-series (blue) and of single-site simulated time-series (red) are shown. The WG models were run 100 times over a 51 year time-period. The numbers (in percentage) indicated above the corresponding model represent the relative deviation of the simulated median from the observed.



1

2 Figure 8. Annual maximum precipitation summed over all eight stations and over consecutive
 3 days. The analysis is done for all days of year. The bars (horizontal line) indicate the range
 4 between the 2.5% and the 97.5% empirical quantiles of the yearly maximum area sums during
 5 1961-2011. The observations are plotted in grey, the multi-site simulations in blue and the
 6 single-site simulations in red. The observations comprise 51 years, the models were run 100
 7 times over a 51 year time-period.